



## **NON-NEWTONIAN FLUID FLOW WITH HEAT TRANSFER THROUGH A POROUS MEDIUM IN A VERTICAL CHANNEL UNDER AN EXTERNAL UNIFORM MAGNETIC FIELD**

**Hamed Mohamed Shawky**

Department of Mathematics

Faculty of (Girls) Al-Azhar University

Nasr City, Cairo, Egypt

### **Abstract**

The problem of the magnetohydrodynamic non-Newtonian fluid flow with heat transfer through a porous medium in a vertical channel is studied. The non-Newtonian fluid under consideration is obeying the rheological equation of state due to Casson model. The system is stressed by a uniform transverse magnetic field. The system of nonlinear partial differential equations which controlled this flow is solved by using Lighthill method. The velocity and temperature distributions are obtained. The effects of various physical parameters of the problem on these distributions are discussed numerically and illustrated graphically through a set of graphs. Also, some special cases are discussed.

### **1. Introduction**

The study of the influence of heat transfer on non-Newtonian fluid has become important in the last few years. This importance is due to a number of industrial processes. Examples are food processing, biochemical operations, transport in polymers, heat exchanger and reactor cooling, beside biomathematical applications such as the flowing of the human blood through arteries.

---

© 2011 Pushpa Publishing House

Keywords and phrases: non-Newtonian fluid, heat transfer, Lighthill method.

Received February 12, 2011

On the other hand many fluids involved in practical applications present a non-Newtonian behavior. Such practical applications in porous media could be encountered in fields like ceramics production, filtration and Oil recovery, certain separation processes, polymer engineering, petroleum production.

Several studies of the magnetohydrodynamic flow with heat transfer through a porous medium over a stretching sheet have been done. Eldabe and Oaf [1] studied the problem of Darcy-Lap wood-Brinkman fluid flow and heat transfer through porous medium over a stretching porous sheet. Magnetohydrodynamic flow of non-Newtonian viscoelastic fluid through a porous medium near an accelerated plate is studied by Eldabe et al. [2]. Also, Eldabe et al. studied the problem of unsteady magnetic boundary layer flow of power law non-Newtonian conducting fluid through a porous medium past an infinite porous flat plate [3]. Eldabe and Sallam [4] studied non-Darcy Couette flow through a porous medium of magnetohydrodynamic viscoelastic fluid with heat and mass transfer. Lie group analysis of unsteady MHD three-dimensional by natural convection from an inclined stretching surface saturated porous medium is studied by EL-Kabeir et al. [5]. Chamkha [6, 7] has investigated the problem of steady and unsteady states, respectively, of laminar, hydromagnetic, three-dimensional free convection flow over a vertical stretching surface in the presence of heat generation or absorption effects. Also some works concerning hydromagnetic flows and heat transfer of electrically conducting fluids over a stretching surface can be found in the papers [8-12]. Also, there are some authors who considered Casson fluid in their works [13] and [14]. Heat and mass transfer in hydrodynamic flow of the viscoelastic fluid over a stretching sheet is studied by Ming [15], in the absence of heat generating effect.

The main idea of this work is to study the mathematical analysis of the Magnetohydrodynamic (MHD) non-Newtonian dusty fluid obeying Casson model and flowing flow in a vertical channel, in the presence of magnetic field with heat transfer. Also to show the relation between the different parameters of the motion and external forces, in order to investigate how to control the motion of the fluid by changing these parameters and external forces. Some of the applications concerning this idea are the flow of oil under ground where there is a natural magnetic field. The other example is the motion of the blood through the arteries.

## 2. Formulation of the Problem

Consider the two-dimensional steady motion of an electrically conducting Casson fluid through a porous medium in a vertical channel in the presence of

external magnetic field. Choose Cartesian coordinates  $(X, Y)$ , where  $X$  axis is in the direction parallel to the walls and  $Y$  axis is perpendicular to it (see Figure 1). The magnetic field of strength  $B_0$  is applied across the channel. We take in our consideration the effects of heat generation, with joules term.

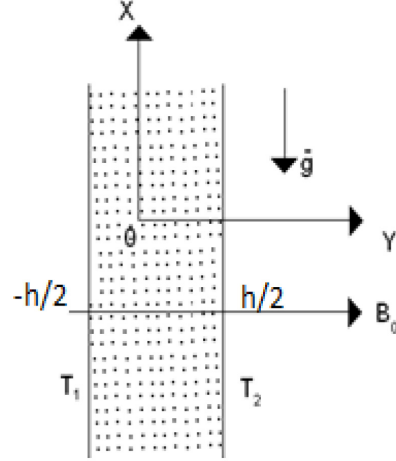


**Figure 1.** Sketch of the problem.

The rheological equation of state for an isotropic and incompressible Casson fluid can be written as [16],

$$\tau_{ij} = \begin{cases} 2 \left[ \mu_B + \frac{p_y}{\sqrt{2\pi}} \right] e_{ij}, & \pi \succ \pi_c \\ 2 \left[ \mu_B + \frac{p_y}{\sqrt{2\pi_c}} \right] e_{ij}, & \pi \prec \pi_c \end{cases},$$

where  $\tau_{ij}$  is the fluid stress,  $e_{ij}$  is the  $(i, j)$ th component of the deformation rate and  $\pi = e_{ij}e_{ij}$ ,  $\pi_c$  is a critical value of this product based on the non-Newtonian model,  $\mu_B$  is plastic dynamic viscosity of the non-Newtonian fluid, and  $p_y$  is yield stress of fluid.

### 3. Equations of Motion

(i) The continuity equation in Cartesian coordinates takes the form

$$\frac{\partial U}{\partial X} + \frac{\partial V}{\partial Y} = 0, \quad (1)$$

where  $U$  and  $V$  are the velocity components in  $X$  and  $Y$  directions respectively, since  $U$  is a function of  $Y$  only, hence, equation (1) becomes  $\partial V / \partial Y = 0$ , this means that  $V$  is constant in any channel section and  $V = 0$  at  $Y = \pm h/2$ .

(ii) The momentum equation has the following components:

$$0 = -\frac{1}{\rho_0} \frac{dP}{dX} + \nu(1 + \lambda^{-1}) \frac{d^2 U}{dY^2} - \frac{\sigma_e B_0^2 U}{\rho_0} - \nu \frac{U}{K} + g\beta(T - T_0), \quad (2)$$

$$0 = -\frac{1}{\rho_0} \frac{\partial P}{\partial Y}. \quad (3)$$

The Oberbeck-Boussinesq approximation is assumed to hold and for the evaluation of the gravitational body force, the density is assumed to depend on temperature according to the equation of state  $\rho = \rho_0 \{1 - \beta(T - T_0)\}$ .

Here  $\nu = \frac{\mu}{\rho_0}$  is the kinematic viscosity,  $\rho_0$  is the density,  $\mu$  is the dynamic viscosity,  $\sigma_e$  is the electrical conductivity of fluid,  $K$  is permeability of the porous medium,  $B_0$  is the magnetic strength,  $g$  is acceleration due to gravity,  $\beta$  is thermal expansion coefficient,  $\lambda = \frac{\mu_B \sqrt{2\pi_c}}{P_y}$  is non-Newtonian parameter,  $P$  is the fluid pressure,  $T$  is the fluid temperature,  $T = T_1$  at  $Y = -h/2$ ,  $T = T_2$  at  $h/2$ ,  $T_0$  is the reference temperature and  $P = \rho_0 gX + p$  is the difference between the pressure and the hydrostatic pressure.

Hence, equation (2) can be written as

$$(1 + \lambda^{-1}) \frac{d^2 U}{dY^2} = \frac{1}{\mu} \frac{dP}{dX} + \frac{\sigma_e B_0^2 U}{\mu} + \frac{U}{K} - \frac{g\beta(T - T_0)}{\nu}. \quad (4)$$

Since the velocity  $U$  and temperature  $T$  are functions of  $Y$  only, if we differentiate (4) with respect to  $X$  we have  $\frac{\partial^2 P}{\partial X^2} = 0$ , and  $\frac{dP}{dX} = \text{constant} = A$ , say therefore equation (4) can be written as

$$(1 + \lambda^{-1}) \frac{d^2 U}{dY^2} = \frac{A}{\mu} + \left( \frac{\sigma_e B_0^2}{\mu} + \frac{1}{K} \right) U - \frac{g\beta(T - T_0)}{\nu}. \quad (5)$$

(iii) The heat equation of the fluid can be written as

$$0 = \alpha \frac{d^2 T}{dY^2} + \frac{\nu(1 + \lambda^{-1})}{C_p} \left( \frac{dU}{dY} \right)^2 + \frac{\sigma_e B_0^2 U^2}{\rho_0 C_p} + \frac{Q^*}{\rho_0 C_p} (T - T_0), \quad (6)$$

where  $\alpha = \frac{k}{\rho_0 C_p}$  is the thermal diffusivity,  $k$  is the thermal conductivity,  $C_p$  is specific heat at constant pressure and  $Q^*$  is a constant which may take either positive or negative values when  $Q^* > 0$  represents the heat source while  $Q^* < 0$  represents the heat sink.

The coupled equations (5) and (6) allow one to obtain a differential equation for  $U$ , namely,

$$\begin{aligned} \frac{d^4 U}{dY^4} = & \left[ \frac{\sigma_e B_0^2}{\rho_0(1 + \lambda^{-1})\nu} + \frac{1}{(1 + \lambda^{-1})K} - \frac{Q^*}{\alpha \rho_0 C_p} \right] \frac{d^2 U}{dY^2} \\ & + \frac{g\beta}{\alpha C_p} \left( \frac{dU}{dY} \right)^2 + \frac{g\beta \sigma_e B_0^2}{\alpha \rho_0 C_p (1 + \lambda^{-1})\nu} U^2 \\ & + \frac{Q^*}{\alpha \rho_0 C_p (1 + \lambda^{-1})\nu} \left[ \frac{\sigma_e B_0^2}{\rho_0} + \frac{\nu}{K} \right] U + \frac{Q^* A}{\rho_0^2 C_p \alpha (1 + \lambda^{-1})\nu}. \end{aligned} \quad (7)$$

The appropriate boundary conditions are

$$U = 0 \quad \text{at} \quad Y = h/2, -h/2, \quad (8)$$

$$\begin{aligned} \frac{d^2 U}{dY^2} = & \frac{A}{\mu(1 + \lambda^{-1})} - \frac{\beta g(T_2 - T_0)}{\nu(1 + \lambda^{-1})} \quad \text{at} \quad Y = h/2, \\ \frac{d^2 U}{dY^2} = & \frac{A}{\mu(1 + \lambda^{-1})} - \frac{\beta g(T_1 - T_0)}{\nu(1 + \lambda^{-1})} \quad \text{at} \quad Y = -h/2. \end{aligned} \quad (9)$$

The following quantities are employed for writing equations (6)-(9) in the dimensionless form

$$u = \frac{U}{U_0}, \quad \theta = \frac{T - T_0}{\Delta T}, \quad y = \frac{Y}{D}, \quad M = \frac{\sigma_e B_0^2 D^2}{\mu(1 + \lambda^{-1})}, \quad G_R = \frac{G_r}{R_e},$$

$$R_e = \frac{U_0 D}{\nu(1 + \lambda^{-1})}, P_r = \frac{\nu(1 + \lambda^{-1})}{\alpha}, B_r = \frac{\mu(1 + \lambda^{-1})U_0^2}{k\Delta T},$$

$$Q = \frac{Q^* D^2}{k}, G_r = \frac{g\beta\Delta T D^3}{\nu^2(1 + \lambda^{-1})^2}, R_t = \frac{T_2 - T_1}{\Delta T}, K_0 = \frac{K}{D^2}, \quad (10)$$

where  $R_t$  is temperature difference ratio,  $G_R$  is dimensionless parameter,  $G_r$  is Grashof number,  $R_e$  is Reynolds number,  $P_r$  is Prandtl number,  $B_r$  is Brinkman number,  $T_1, T_2$  are the prescribed boundary temperatures,  $M$  is the magnetic parameter and  $D = 2$ ,  $h$  is the hydraulic diameter. The reference velocity  $U_0$ , the reference temperature  $T_0$  and the reference temperature difference  $\Delta T$  are given by

$$U_0 = -\frac{AD^2}{48\mu(1 + \lambda^{-1})}, \quad T_0 = \frac{T_1 + T_2}{2},$$

$$\Delta T = T_2 - T_1 \quad \text{if} \quad T_1 \prec T_2, \quad \Delta T = \frac{\nu^2(1 + \lambda^{-1})^2}{D^2 C_P} \quad \text{if} \quad T_1 = T_2. \quad (11)$$

The dimensionless parameter  $R_T$  becomes zero for symmetric heating ( $T_1 = T_2$ ) and one for asymmetric heating ( $T_1 \prec T_2$ ).

Using equation (10), equations (6)-(9) become

$$\frac{d^4 u}{dy^4} - N_1 \frac{d^2 u}{dy^2} - N_2 u - N_3 = G_R B_r \left( \frac{du}{dy} \right)^2 + M G_R B_r u^2, \quad (12)$$

$$\frac{d^2 \theta}{dy^2} + Q\theta = -B_r \left( \frac{du}{dy} \right)^2 - B_r M u^2, \quad (13)$$

where

$$N_1 = \left\{ M + \frac{1}{K_0(1 + \lambda^{-1})} - Q \right\},$$

$$N_2 = Q \left[ M + \frac{1}{K_0(1 + \lambda^{-1})} \right], \quad N_3 = -48Q \quad (14)$$

with the boundary conditions

$$\begin{aligned}
 u &= 0 & \text{at } y &= 1/4, -1/4, \\
 \theta &= \frac{R_t}{2} & \text{at } y &= 1/4, \quad \theta = -\frac{R_t}{2} & \text{at } y &= -1/4, \\
 \frac{d^2 u}{dy^2} &= -48 - \frac{R_t G_R}{2} & \text{at } y &= 1/4, \\
 \frac{d^2 u}{dy^2} &= -48 + \frac{R_t G_R}{2} & \text{at } y &= -1/4.
 \end{aligned} \tag{15}$$

#### Notice that

For an ordinary non-Newtonian fluid ( $\lambda \rightarrow \infty$ ), and in the absence of heat generating ( $Q = 0$ ) with non-porous medium ( $K \rightarrow \infty$ ), the system of our equations leads to the system which treated by [17].

**Case [1].**  $B_r = 0$  (when the viscous dissipation is negligible).

Equations (12) and (13) for velocity  $u$  and temperature  $\theta$  become uncoupled and they can be solved with boundary conditions (15), then we have

$$u = A \cosh \alpha_1 y + B \sinh \alpha_1 y + \chi \cosh \beta_1 y + \Gamma \sinh \beta_1 y - N_4, \tag{16}$$

$$\theta = \frac{R_t}{2 \sin m_0/4} \sin m_0 y, \tag{17}$$

where

$$\begin{aligned}
 Q &= m_0^2, \quad \alpha_1^2 = \frac{N_1 + \sqrt{N_1^2 + 4N_2}}{2}, \quad \beta_1^2 = \frac{N_1 - \sqrt{N_1^2 + 4N_2}}{2}, \\
 A &= \frac{-(48 + N_4 \beta_1^2)}{(\alpha_1^2 - \beta_1^2) \cosh \alpha_1/4}, \quad \chi = \frac{(48 + N_4 \alpha_1^2)}{(\alpha_1^2 - \beta_1^2) \cosh \beta_1/4}, \quad N_4 = \frac{N_3}{N_2}, \\
 B &= \frac{-(G_R R_t)}{2(\alpha_1^2 - \beta_1^2) \sinh \alpha_1/4}, \quad \Gamma = \frac{(G_R R_t)}{2(\alpha_1^2 - \beta_1^2) \sinh \beta_1/4}.
 \end{aligned} \tag{18}$$

#### Notice that

In the case of symmetric heating, when buoyancy forces are dominating, i.e., when  $G_R \rightarrow \pm\infty$ , equation (16) gives

$$\frac{u}{G_R} = B \sinh \alpha_1 y + \Gamma \sinh \beta_1 y. \tag{19}$$

**Case [2].**  $G_R = 0$  (which means the buoyancy forces are negligible and viscous dissipation is relevant). Solutions of equations (12) and (13) by using boundary conditions (15) become

$$u = A \cosh \alpha_1 y + \chi \cosh \beta_1 y - N_4, \quad (20)$$

$$\begin{aligned} \theta = & L_1 \left\{ \left( \frac{\cos m_0 y}{\cos m_0/4} \right) \cosh \alpha_1/2 - \cosh 2\alpha_1 y \right\} \\ & + L_2 \left\{ \left( \frac{\cos m_0 y}{\cos m_0/4} \right) \cosh \beta_1/2 - \cosh 2\beta_1 y \right\} \\ & + L_3 \left\{ \cosh (\alpha_1 - \beta_1) y - \left( \frac{\cos m_0 y}{\cos m_0/4} \right) \cosh (\alpha_1 - \beta_1)/4 \right\} \\ & + L_4 \left\{ \cosh \alpha_1 y - \left( \frac{\cos m_0 y}{\cos m_0/4} \right) \cosh \alpha_1/4 \right\} \\ & + L_5 \left\{ \cosh (\alpha_1 + \beta_1) y - \left( \frac{\cos m_0 y}{\cos m_0/4} \right) \cosh (\alpha_1 + \beta_1)/4 \right\} \\ & + L_6 \left\{ \cosh \beta_1 y - \left( \frac{\cos m_0 y}{\cos m_0/4} \right) \cosh \beta_1/4 \right\} \\ & + L_7 \left\{ 1 - \left( \frac{\cos m_0 y}{\cos m_0/4} \right) \right\} + \frac{R_T}{2 \sin m_0/4} \sin m_0 y, \end{aligned} \quad (21)$$

where

$$\begin{aligned} L_1 &= \frac{B_r A^2 (M + \alpha_1^2)}{2(m_0^2 + 4\alpha_1^2)}, \quad L_2 = \frac{B_r \chi^2 (M + \beta_1^2)}{2(m_0^2 + 4\beta_1^2)}, \\ L_3 &= \frac{B_r A \chi (\alpha_1 \beta_1 - M)}{(\alpha_1 - \beta_1)^2 + m_0^2}, \quad L_4 = \frac{2B_r A M N_4}{(m_0^2 + \alpha_1^2)}, \\ L_5 &= \frac{B_r A \chi (-\alpha_1 \beta_1 - M)}{(\alpha_1 + \beta_1)^2 + m_0^2}, \quad L_6 = \frac{2B_r \chi M N_4}{(m_0^2 + \beta_1^2)}, \\ L_7 &= \frac{B_r}{2m_0^2} [A^2 \alpha_1^2 + \chi^2 \beta_1^2 - M(A^2 + \chi^2 + 2N_4^2)]. \end{aligned} \quad (22)$$



#### 4. Perturbation Method

In order to the coupled nonlinear differential equations (12) and (13) we can use the following perturbation series method [18] for the velocity and temperature distribution can be written

$$u = u_0(y) + \varepsilon u_1(y) + O(\varepsilon^2) + \cdots = \sum_{n=0}^{\infty} \varepsilon^n u_n(y), \quad (23)$$

$$\theta = \theta_0(y) + \varepsilon \theta_1(y) + O(\varepsilon^2) + \cdots = \sum_{n=0}^{\infty} \varepsilon^n \theta_n(y), \quad (24)$$

where

$$\varepsilon = B_r G_R = R_e P_r L \quad (25)$$

and

$$\frac{\beta g D}{C_p} = L.$$

Substituting these equations (23) and (24) into equations (12) and (13) and equating the coefficient of like powers of  $\varepsilon$  for  $n = 0$  and  $n = 1$  and neglecting the terms beginning from  $n = 2$  and higher, we get the following pairs of equations:

$$\frac{d^4 u_0}{dy^4} - N_1 \frac{d^2 u_0}{dy^2} - N_2 u_0 - N_3 = 0, \quad (26)$$

$$\frac{d^4 u_1}{dy^4} - N_1 \frac{d^2 u_1}{dy^2} - N_2 u_1 = \left( \frac{du_0}{dy} \right)^2 + M u_0^2, \quad (27)$$

$$\frac{d^2 \theta_0}{dy^2} + Q \theta_0 = 0, \quad (28)$$

$$\frac{d^2 \theta_1}{dy^2} + Q \theta_1 = -\frac{1}{G_R} \left( \frac{du_0}{dy} \right)^2 - \frac{M}{G_R} B_r u_0^2. \quad (29)$$

The corresponding conditions can be written

$$\begin{aligned}
 u_0 = 0, \quad u_1 = 0, \quad \theta_1 = 0 & \quad \text{at } y = 1/4, -1/4, \\
 \theta_0 = \frac{R_t}{2} \quad \text{at } y = 1/4, & \quad \theta_0 = -\frac{R_t}{2} \quad \text{at } y = -1/4, \\
 \frac{d^2 u_0}{dy^2} = -48 - \frac{R_t G_R}{2}, \quad \frac{d^2 u_1}{dy^2} = 0 & \quad \text{at } y = 1/4, \\
 \frac{d^2 u_0}{dy^2} = -48 + \frac{R_t G_R}{2}, \quad \frac{d^2 u_1}{dy^2} = 0 & \quad \text{at } y = -1/4.
 \end{aligned} \tag{30}$$

Hence, the solution of equations (26)-(29) corresponding the conditions (30) can be written as

$$\begin{aligned}
 u = & A \cosh \alpha_1 y + B \sinh \alpha_1 y + \chi \cosh \beta_1 y + \Gamma \sinh \beta_1 y - N_4 \\
 & + \varepsilon \{ [C_1 \cosh \alpha_1 y C_2 \sinh \alpha_1 y + C_3 \cosh \beta_1 y + C_4 \sinh \beta_1 y + C_5 \\
 & + H_1 [(A^2 + B^2) \cosh 2\alpha_1 y + 2AB \sinh 2\alpha_1 y] \\
 & + H_2 [(\chi^2 + \Gamma^2) \cosh 2\beta_1 y + 2\chi\Gamma \sinh 2\beta_1 y] \\
 & + H_3 [(B\Gamma + A\chi) \cosh(\alpha_1 + \beta_1)y + (B\chi + A\Gamma) \sinh(\alpha_1 + \beta_1)y] \\
 & + H_4 \cosh(\alpha_1 - \beta_1)y + H_5 \sinh(\alpha_1 - \beta_1)y \\
 & - H_6 [A \cosh \alpha_1 y + B \sinh \alpha_1 y] - H_7 [\chi \cosh \beta_1 y + \Gamma \sinh \beta_1 y] \}, \tag{31}
 \end{aligned}$$

where

$$\begin{aligned}
 H_1 &= \frac{\alpha_1^2 + M}{2(16\alpha_1^4 - 4N_1\alpha_1^2 - N_2)}, \quad H_2 = \frac{M + \beta_1^2}{2(16\beta_1^4 - 4N_1\beta_1^2 - N_2)}, \\
 H_3 &= \frac{\alpha_1\beta_1 + M}{(\alpha_1 + \beta_1)^4 - N_1(\alpha_1 + \beta_1)^2 - N_2}, \quad H_6 = \frac{2N_4M}{\alpha_1^4 - N_1\alpha_1^2 - N_2}, \\
 H_4 &= \frac{(A\chi - B\Gamma)(M - \alpha_1\beta_1)}{(\alpha_1 - \beta_1)^4 - N_1(\alpha_1 - \beta_1)^2 - N_2}, \quad H_7 = \frac{2N_4M}{\beta_1^4 - N_1\beta_1^2 - N_2}, \\
 H_5 &= \frac{(A\Gamma + B\chi)(M + \alpha_1\beta_1)}{(\alpha_1 - \beta_1)^4 - N_1(\alpha_1 - \beta_1)^2 - N_2}, \tag{32}
 \end{aligned}$$

and

$$C_5 = \frac{1}{2N_2} \{(\Gamma^2 - \chi^2)(\beta_1^2 + M) + (A^2 - B^2)(\alpha_1^2 - M) - 2N_4^2 M\}, \quad (33)$$

$$\begin{aligned} C_1 = & \frac{1}{(\beta_1^2 - \alpha_1^2) \cosh \alpha_1} [-C_5 \beta_1^2 - H_1(A^2 + B^2)(\beta_1^2 - 4\alpha_1^2) \cosh 2\alpha_1 \\ & + H_2\{3(\chi^2 + \Gamma^2)\beta_1^2 \cosh 2\beta_1\} \\ & - H_3(B\Gamma + A\chi)(\beta_1^2 - (\alpha_1 + \beta_1)^2) \cosh(\alpha_1 + \beta_1) \\ & - H_4(\beta_1^2 - (\alpha_1 - \beta_1)^2) \cosh(\alpha_1 - \beta_1) + H_6 A], \end{aligned} \quad (34)$$

$$\begin{aligned} C_2 = & \frac{1}{(\beta_1^2 - \alpha_1^2) \sinh \alpha_1} [-H_1 AB(2\beta_1^2 - 8\alpha_1^2) \sinh 2\alpha_1 \\ & + H_2\{6\chi\Gamma\beta_1^2 \sinh 2\beta_1\} - H_3(B\chi + A\Gamma)(\beta_1^2 - (\alpha_1 + \beta_1)^2) \sinh(\alpha_1 + \beta_1) \\ & - H_5(\beta_1^2 - (\alpha_1 - \beta_1)^2) \sinh(\alpha_1 - \beta_1) + H_6 B], \end{aligned} \quad (35)$$

$$\begin{aligned} C_3 = & \frac{-1}{(\beta_1^2 - \alpha_1^2) \cosh \beta_1} [-C_5 \alpha_1^2 + 3H_1(A^2 + B^2)\alpha_1^2 \cosh 2\alpha_1 \\ & - H_2\{(\chi^2 + \Gamma^2)(\alpha_1^2 - 4\beta_1^2) \cosh 2\beta_1\} \\ & - H_3(B\Gamma + A\chi)(\alpha_1^2 - (\alpha_1 + \beta_1)^2) \cosh(\alpha_1 + \beta_1) \\ & - H_4(\alpha_1^2 - (\alpha_1 - \beta_1)^2) \cosh(\alpha_1 - \beta_1) + H_7 C], \end{aligned} \quad (36)$$

$$\begin{aligned} C_4 = & \frac{-1}{(\beta_1^2 - \alpha_1^2) \sinh \beta_1} [6H_1 AB\alpha_1^2 \sinh 2\alpha_1 \\ & - H_5(\beta_1^2 - (\alpha_1 - \beta_1)^2) \sinh(\alpha_1 - \beta_1) H_2\{\chi\Gamma(2\alpha_1^2 - 8\beta_1^2)\beta_1^2 \sinh 2\beta_1\} \\ & - H_3(B\chi + A\Gamma)(\alpha_1^2 - (\alpha_1 + \beta_1)^2) \sinh(\alpha_1 + \beta_1) + H_7 D], \end{aligned} \quad (37)$$

$$\begin{aligned} \theta = & \frac{R_t}{2 \sin m_0} \sin m_0 y + \frac{\varepsilon}{G_R} \left[ \left\{ E_1 \left\{ \left( \frac{\cos m_0 y}{\cos m_0} \right) \cosh 2\alpha_1 - \cosh 2\alpha_1 y \right\} \right. \right. \\ & \left. \left. + E_2 \left\{ \left( \frac{\sin m_0 y}{\sin m_0} \right) \sinh 2\alpha_1 - \sinh 2\alpha_1 y \right\} \right. \right. \end{aligned}$$

$$\begin{aligned}
& + E_3 \left\{ \left( \frac{\cos m_0 y}{\cos m_0} \right) \cosh(\alpha_1 + \beta_1) - \cosh(\alpha_1 + \beta_1) y \right\} \\
& + E_4 \left\{ \left( \frac{\cos m_0 y}{\cos m_0} \right) \cosh(\alpha_1 - \beta_1) - \cosh(\alpha_1 - \beta_1) y \right\} \\
& + E_5 \left\{ \left( \frac{\sin m_0 y}{\sin m_0} \right) \sinh(\alpha_1 + \beta_1) - \sinh(\alpha_1 + \beta_1) y \right\} \\
& + E_6 \left\{ \left( \frac{\sin m_0 y}{\sin m_0} \right) \sinh(\alpha_1 - \beta_1) - \sinh(\alpha_1 - \beta_1) y \right\} \\
& + E_7 \left\{ \left( \frac{\cos m_0 y}{\cos m_0} \right) \cosh 2\beta_1 - \cosh 2\beta_1 y \right\} \\
& + E_8 \left\{ \left( \frac{\sin m_0 y}{\sin m_0} \right) \sinh 2\beta_1 - \sinh 2\beta_1 y \right\} \\
& + E_9 \left\{ \cosh \alpha_1 y - \left( \frac{\cos m_0 y}{\cos m_0} \right) \cosh \alpha_1 \right\} \\
& + E_{10} \left\{ \cosh \beta_1 y - \left( \frac{\cos m_0 y}{\cos m_0} \right) \cosh \beta_1 \right\} \\
& + E_{11} \left\{ \sinh \alpha_1 y - \left( \frac{\sin m_0 y}{\sin m_0} \right) \sinh \alpha_1 \right\} \\
& + E_{12} \left\{ \sinh \beta_1 y - \left( \frac{\sin m_0 y}{\sin m_0} \right) \sinh \beta_1 \right\} \\
& + E_{13} \left[ \left\{ \left( \frac{\cos m_0 y}{\cos m_0} \right) - 1 \right\} \right], \tag{38}
\end{aligned}$$

where

$$\begin{aligned}
E_1 &= \frac{(A^2 + B^2)(M + \alpha_1^2)}{2(4\alpha_1^2 + m_0^2)}, & E_2 &= \frac{AB(M + \alpha_1^2)}{(m_0^2 + 4\alpha_1^2)}, \\
E_3 &= \frac{(B\Gamma + A\chi)(\alpha_1\beta_1 + M)}{m_0^2 + (\alpha_1 + \beta_1)^2}, & E_4 &= \frac{(B\Gamma + A\chi)(\alpha_1\beta_1 + M)}{m_0^2 + (\alpha_1 - \beta_1)^2},
\end{aligned}$$

$$\begin{aligned}
E_5 &= \frac{(B\chi + A\Gamma)(\alpha_1\beta_1 + M)}{m_0^2 + (\alpha_1 + \beta_1)^2}, & E_9 &= \frac{2AMN_4}{(m_0^2 + \alpha_1^2)}, \\
E_6 &= \frac{(B\chi + A\Gamma)(\alpha_1\beta_1 + M)}{m_0^2 + (\alpha_1 - \beta_1)^2}, & E_7 &= \frac{(\Gamma^2 + \chi^2)(M + \beta_1^2)}{2(4\beta_1^2 + m_0^2)}, \\
E_8 &= \frac{\Gamma\chi(M + \beta_1^2)}{(m_0^2 + 4\beta_1^2)}, & E_{10} &= \frac{2\chi MN_4}{(m_0^2 + \beta_1^2)}, \\
E_{11} &= \frac{2BMN_4}{(m_0^2 + \alpha_1^2)}, & E_{12} &= \frac{2\Gamma MN_4}{(m_0^2 + \beta_1^2)}, \\
E_{13} &= \frac{1}{2m_0^2} [(A^2 - B^2)(M - \alpha_1^2) + (\chi^2 - \Gamma^2)(M - \beta_1^2) + 2N_4^2 M]. \quad (39)
\end{aligned}$$

## 5. Discussion

In this paper, we obtained analytically the velocity and temperature distributions for the steady motion of an electrically conducting Casson fluid through a porous medium in a vertical channel. The effects of the physical problem on numerical calculating of these formulae are discussed and illustrated graphically through Figures 2-28.

1. The following figures are illustrated for the case  $B_r = 0$ .

Figure 2 shows the relation between the velocity component  $u$  and the Magnetic parameter  $M$ . It is clear that the velocity  $u$  decreases with increasing  $M$ .

Figure 3 shows the effect of the non-Newtonian parameter  $\lambda$  on the velocity field. It is clear that the velocity  $u$  decreases with increasing  $\lambda$ .

In Figure 4, the relation between the velocity component  $u$  and the porous medium parameter  $K_0$  is illustrated. It is clear that the velocity  $u$  increases with increasing  $K_0$ .

In Figure 5, the effect of the heat source parameter  $Q$  on the velocity field is illustrated. It is seen that the velocity decreases with increasing  $Q$  in the region from  $y = -0.25$  up to  $y = 0$ , and the increases from  $y = 0$  to  $y = 0.25$ .

The effect of the temperature difference ratio  $R_T$  on velocity field is discussed through Figure 6. It is seen that the velocity decreases and increases with increasing  $R_T$ .

The effect of the parameter  $G_R = \frac{G_r}{R_e}$  on velocity field in the case of asymmetric heating ( $R_T = 1$ ) is discussed through Figure 7. It is seen that the velocity decreases and increases with increasing  $G_R$ .

In Figure 8, the effect of the heat source parameter  $Q$  on the temperature distribution is illustrated. It is seen that the temperature decreases and increases with increasing  $Q$ .

**2.** The following figures are illustrated for the case  $G_R = 0$ .

Figure 9 shows the relation between the velocity components  $u$  and the Magnetic parameter  $M$ . It is clear that the velocity  $u$  decreases with increasing  $M$ .

Figure 10 shows the effect of the non-Newtonian parameter  $\lambda$  on the velocity field. It is clear that the velocity  $u$  decreases with increasing  $\lambda$ .

In Figure 11, the relation between the velocity components  $u$  and the porous medium parameter  $K_0$  is plotted drawn. It is clear that the velocity  $u$  increases with increasing  $K_0$ .

In Figure 12, the effect of the heat source parameter  $Q$  on the temperature distribution is illustrated. It is seen that the temperature decreases and increases with increasing  $Q$ .

The effect of the of Brinkman number parameter  $B_r$  on the temperature of the Casson model is illustrated in Figure 13. It is seen that the temperature increases with increasing  $B_r$  which shown.

**3.** The following figures are illustrated for the general case.

Figure 14 shows the relation between the velocity component  $u$  and the Magnetic parameter  $M$ . It is clear that the velocity  $u$  decreases with increasing  $M$ .

Figure 15 shows the effect of the non-Newtonian parameter  $\lambda$  on the velocity field. It is clear that the velocity  $u$  decreases with increasing  $\lambda$ .

In Figure 16, the relation between the velocity component  $u$  and the porous medium parameter  $K_0$  is plotted drawn. It is clear that the velocity  $u$  increases with increasing  $K_0$ .

In Figure 17, the effect of the heat source parameter  $Q$  on the velocity field is illustrated. It is seen that the velocity decreases and increases with increasing  $Q$ .

The effect of the Prandtl number parameter  $P_r$  on the velocity of the Casson model is illustrated through Figure 18. It is seen that the velocity increases with increasing  $P_r$ .

The effect of the temperature difference ratio  $R_T$  on velocity field is discussed through Figure 19. It is seen that the velocity decreases and increases with increasing  $R_T$ .

In Figure 20, the effect of the Grashof number parameter  $G_r$  on the velocity field is illustrated. It is seen that the velocity decreases and increases with increasing  $G_r$ .

Figure 21 shows the relation between the temperature field of the fluid and the magnetic parameter  $M$ . It reveals that the temperature increases with increasing  $M$ .

The effect of the non-Newtonian parameter  $\lambda$  on the temperature distribution is discussed through Figure 22. It is seen that the temperature increases with increasing  $\lambda$ .

Figure 23 shows the relation between the temperature of the fluid and the porous medium parameter  $K_0$ . It is clear that the temperature increases with increasing  $K_0$ .

In Figure 24, the effect of the heat source parameter  $Q$  on the temperature distribution is illustrated. It is seen that the temperature increases with increasing  $Q$ .

The effect of the of the Prandtl number parameter  $P_r$  on the temperature of the Casson model is illustrated in Figure 25. It is seen that the temperature increases with increasing  $P_r$  which shown.

In Figure 26, the relation between the temperature of the fluid and the effect of the dimensionless parameter  $G_R = \frac{G_r}{R_e}$ . It is clear that the temperature increases with increasing  $G_R$ .

The effect of the parameter  $\varepsilon = G_R B_r$  on the temperature is discussed through Figure 27. It is seen that the temperature increases with increasing  $\varepsilon$ .

The effect of the Grashof number parameter  $G_r$  on the temperature is discussed through Figure 28. It is seen that the temperature increases with increasing  $G_r$ .

## 6. Conclusion

The mathematical models for momentum and the energy equations which describe the physical phenomena of the magnetohydrodynamic non-Newtonian (Casson fluid flow) with heat and mass transfer through porous medium in a vertical channel are investigated. These equations are solved analytically. The effects of the problem parameters on the solutions are studied. The obtained results were illustrated graphically to show how to control the velocity and heat of the fluid flow. While there is no similar experimental case to this theoretical study, we have only compared our results in special cases with other previous published works, say.

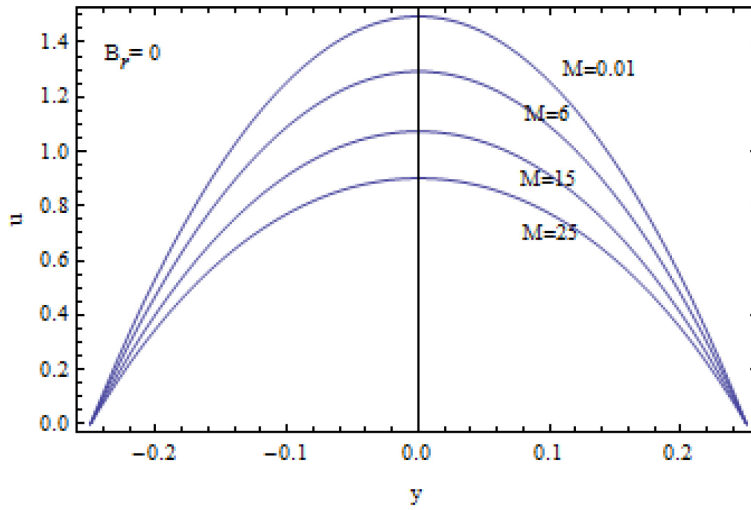


**Figure 2.** The velocity ( $u$ ) of the fluid is drawn against  $y$  for different values of  $M = 0.01, 6, 15, 25$ ,  $Q = 0.01$ ,  $\lambda = 0.01$ ,  $K_0 = 0.1$ ,  $G_R = 0.5$ ,  $R_T = 0.5$ .



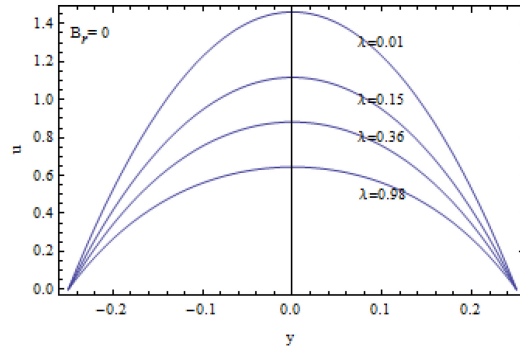


**Figure 3.** The velocity ( $u$ ) of the fluid is drawn against  $y$  for different values of  $\lambda = 0.01, 0.15, 0.36, 0.98$ ,  $Q = 1$ ,  $M = 0.01$ ,  $K_0 = 0.01$ ,  $G_R = 0.5$ ,  $R_T = 0.5$ .

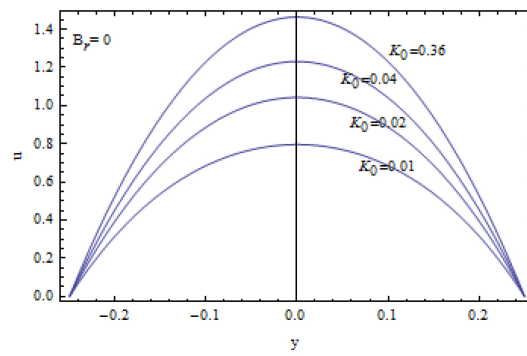


**Figure 4.** The velocity ( $u$ ) of the fluid is drawn against  $y$  for different values of  $K_0 = 0.01, 0.02, 0.04, 0.36$ ,  $Q = 0.01$ ,  $M = 0.01$ ,  $\lambda = 0.5$ ,  $G_R = 0.1$ ,  $R_T = 1$ .

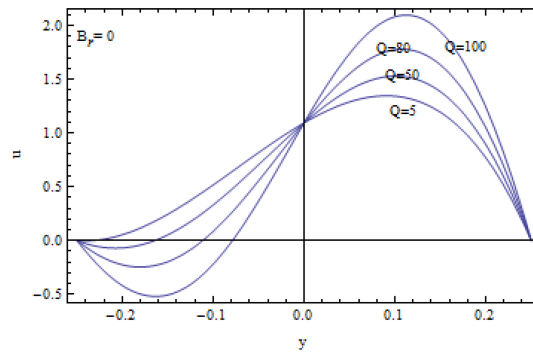


**Figure 5.** The velocity ( $u$ ) of the fluid is drawn against  $y$  for different values of  $Q = 5, 50, 80, 100$ ,  $\lambda = 0.1$ ,  $M = 5$ ,  $K_0 = 0.01$ ,  $G_R = 50$ ,  $R_T = 5$ .

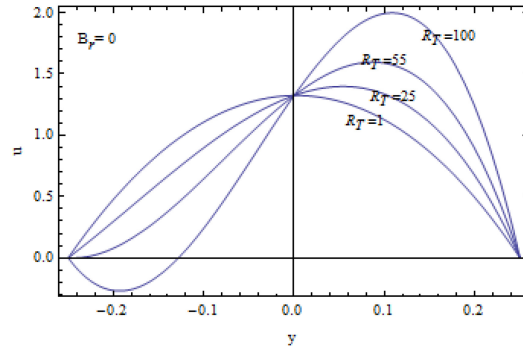


**Figure 6.** The velocity ( $u$ ) of the fluid is drawn against  $y$  for different values of  $R_T = 1, 25, 55, 100$ ,  $\lambda = 0.01$ ,  $M = 5$ ,  $K_0 = 0.1$ ,  $G_R = 5$ ,  $Q = 5$ .

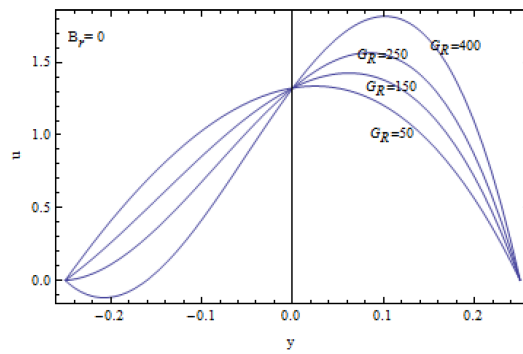


**Figure 7.** The velocity ( $u$ ) of the fluid is drawn against  $y$  for different values of  $G_R = 50, 150, 250, 400$ ,  $\lambda = 0.01$ ,  $M = 5$ ,  $K_0 = 0.1$ ,  $Q = 5$ ,  $R_T = 1$ .

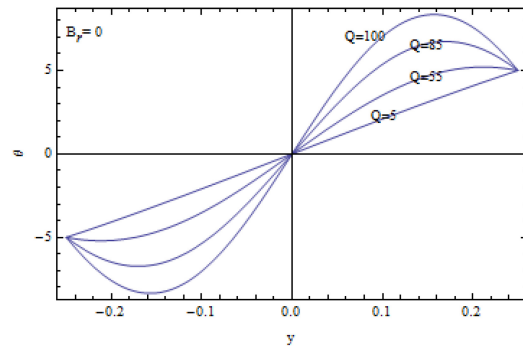


**Figure 8.** The temperature ( $\theta$ ) of the fluid is drawn against  $y$  for different values of  $Q = 5, 55, 85, 100$ ,  $R_T$ .

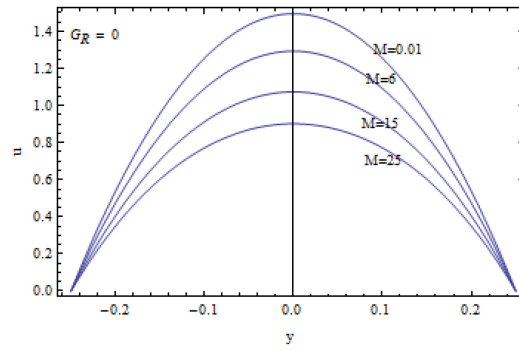


**Figure 9.** The velocity ( $u$ ) of the fluid is drawn against  $y$  for different values of  $M = 0.01, 6, 15, 25$ ,  $Q = 0.01$ ,  $\lambda = 0.01$ ,  $K_0 = 0.1$ .

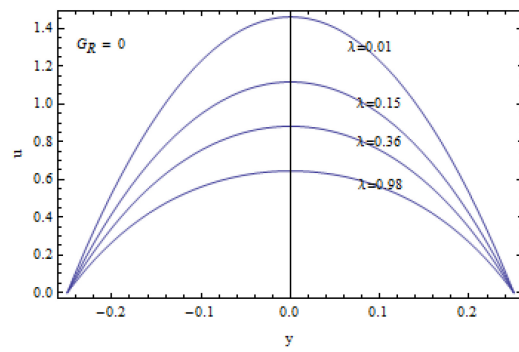


**Figure 10.** The velocity ( $u$ ) of the fluid is drawn against  $y$  for different values of  $\lambda = 0.01, 0.15, 0.36, 0.98$ ,  $Q = 1$ ,  $M = 0.01$ ,  $K_0 = 0.01$ .

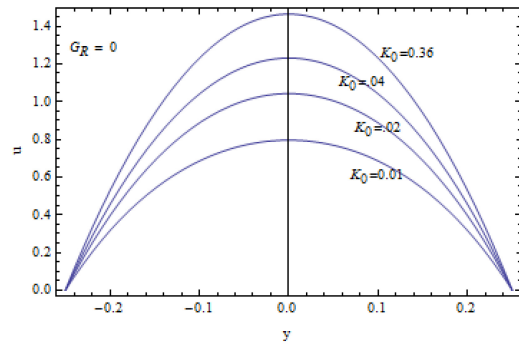


**Figure 11.** The velocity ( $u$ ) of the fluid is drawn against  $y$  for different values of  $K_0 = 0.01, 0.02, 0.04, 0.36$ ,  $Q = 0.01$ ,  $M = 0.01$ ,  $\lambda = 0.5$ .

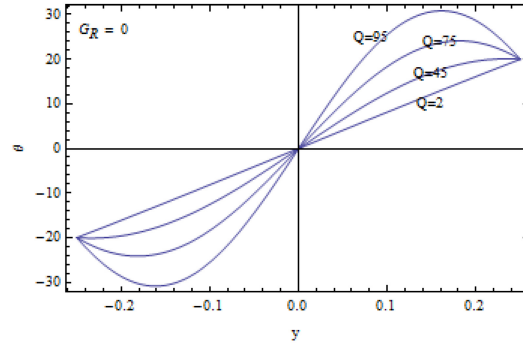


**Figure 12.** The temperature ( $\theta$ ) of the fluid is drawn against  $y$  for different values of  $Q = 5, 45, 75, 95$ ,  $\lambda = 0.2$ ,  $M = 0.2$ ,  $K_0 = 0.1$ ,  $B_r = 0.01$ ,  $R_T = 40$ .

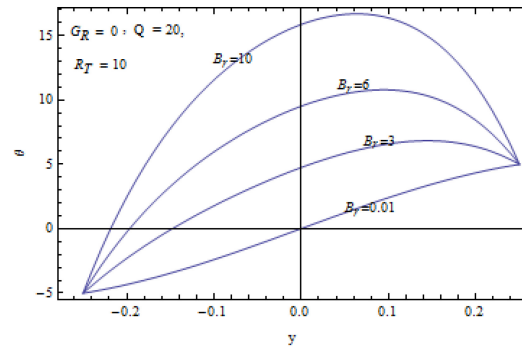


**Figure 13.** The temperature ( $\theta$ ) of the fluid is drawn against  $y$  for different values of  $B_r = 0.01, 3, 6, 10$ ,  $Q = 20$ ,  $\lambda = 0.01$ ,  $M = 2$ ,  $K_0 = 0.01$ ,  $R_T = 10$ .

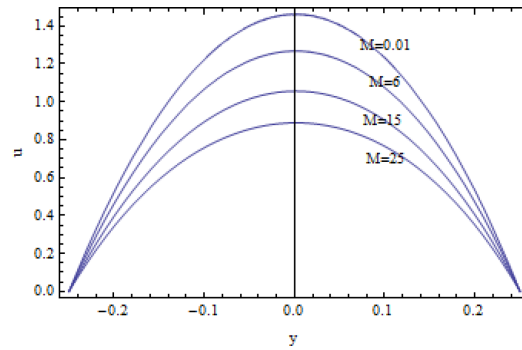


**Figure 14.** The velocity ( $u$ ) of the fluid is drawn against  $y$  for different values of  $M = 0.01, 6, 15, 25$ ,  $Q = 2$ ,  $\lambda = 0.01$ ,  $K_0 = 0.01$ ,  $G_R = 5$ ,  $R_T = 0.5$ ,  $L = 0.1$ ,  $P_r = 0.1$ ,  $R_e = 0.01$ ,  $B_r = 0.01$ .

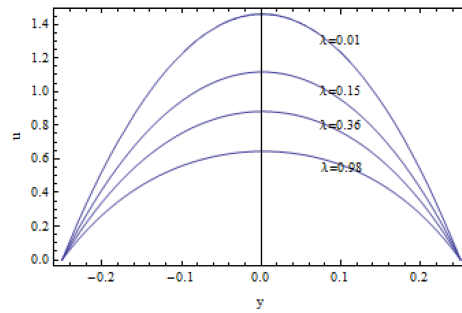


**Figure 15.** The velocity ( $u$ ) of the fluid is drawn against  $y$  for different values of  $\lambda = 0.01, 0.15, 0.36, 0.98$ ,  $Q = 2$ ,  $M = 0.01$ ,  $K_0 = 0.01$ ,  $G_R = 5$ ,  $R_T = 0.5$ ,  $L = 0.1$ ,  $P_r = 0.1$ ,  $R_e = 0.01$ ,  $B_r = 0.01$ .

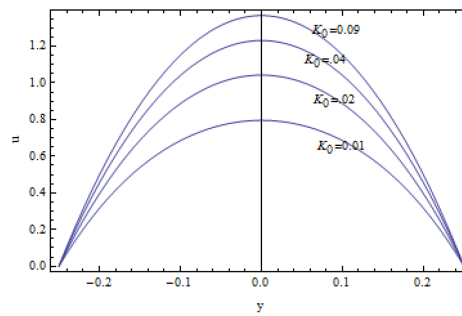


**Figure 16.** The velocity ( $u$ ) of the fluid is drawn against  $y$  for different values of  $K_0 = 0.01, 0.02, 0.04, 0.36$ ,  $Q = 0.01$ ,  $M = 0.01$ ,  $\lambda = 0.5$ ,  $G_R = 0.1$ ,  $R_T = 0.1$ ,  $L = 0.1$ ,  $P_r = 0.1$ ,  $R_e = 0.01$ ,  $B_r = 0.01$ .

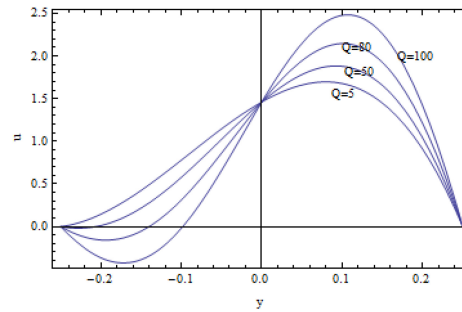


**Figure 17.** The velocity ( $u$ ) of the fluid is drawn against  $y$  for different values of  $Q = 5, 50, 80, 100$ ,  $\lambda = 0.01$ ,  $M = 0.01$ ,  $K_0 = 0.01$ ,  $B_r = 0.05$ ,  $R_T = 5$ ,  $G_R = 50$ ,  $L = 0.1$ ,  $P_r = 0.1$ ,  $R_e = 0.01$ .

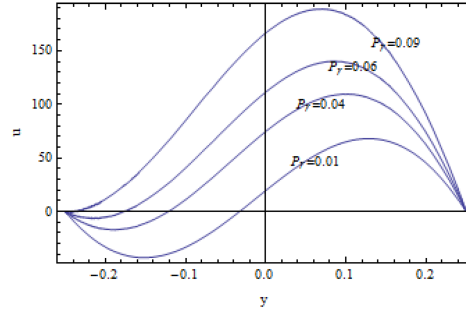


**Figure 18.** The velocity ( $u$ ) of the fluid is drawn against  $y$  for different values of  $P_r = 0.01, 0.04, 0.06, 0.09$ ,  $\lambda = 0.9$ ,  $M = 5$ ,  $K_0 = 0.09$ ,  $B_r = 1$ ,  $R_T = 50$ ,  $G_R = 400$ ,  $L = 1$ ,  $Q = 50$ ,  $R_e = 0.55$ .

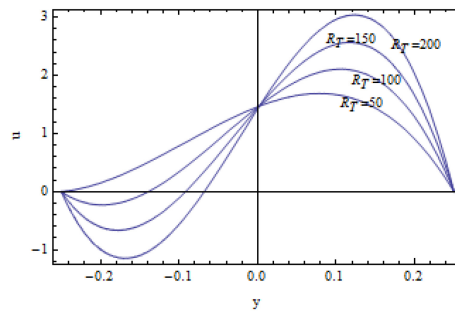


**Figure 19.** The velocity ( $u$ ) of the fluid is drawn against  $y$  for different values of  $R_T = 50, 100, 150, 200$ ,  $P_r = 0.1$ ,  $\lambda = 0.01$ ,  $M = 0.01$ ,  $K_0 = 0.09$ ,  $B_r = 1$ ,  $G_R = 5$ ,  $L = 0.1$ ,  $Q = 2$ ,  $R_e = 0.01$ .

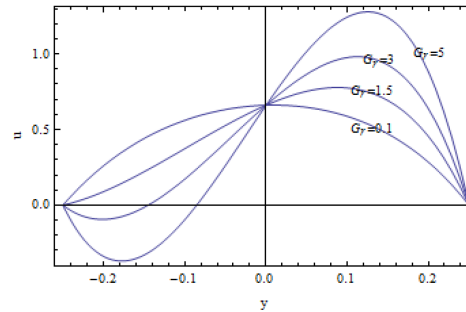


**Figure 20.** The velocity ( $u$ ) of the fluid is drawn against  $y$  for different values of  $G_r = 0.1, 1.5, 3, 5$ ,  $P_r = 0.1$ ,  $\lambda = 0.9$ ,  $M = 0.1$ ,  $K_0 = 0.01$ ,  $B_r = 0.1$ ,  $\varepsilon = 0.01$ ,  $Q = 2.5$ ,  $R_e = 0.01$ ,  $R_T = 1$ .

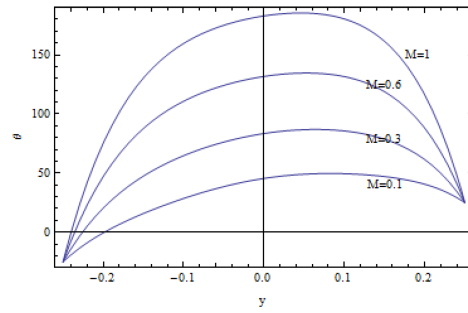


**Figure 21.** The temperature ( $\theta$ ) of the fluid is drawn against  $y$  for different values of  $M = 0.1, 0.3, 0.6, 1$ ,  $Q = 5$ ,  $\lambda = 0.01$ ,  $K_0 = 0.01$ ,  $G_R = 200$ ,  $R_T = 50$ ,  $\varepsilon = 5$ ,  $B_r = 0.5$ .

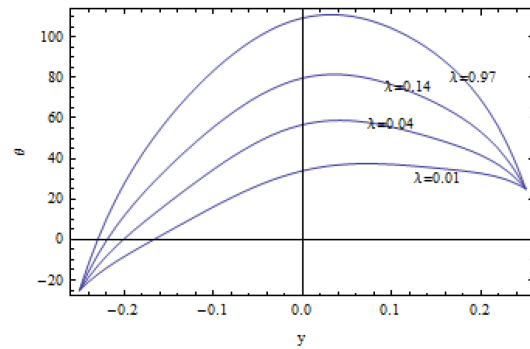


**Figure 22.** The temperature of the fluid is drawn against  $y$  for different values of  $\lambda = 0.01, 0.04, 0.14, 0.97$ ,  $Q = 5$ ,  $M = 0.1$ ,  $K_0 = 0.01$ ,  $G_R = 300$ ,  $R_T = 50$ ,  $\varepsilon = 8$ ,  $B_r = 0.5$ .

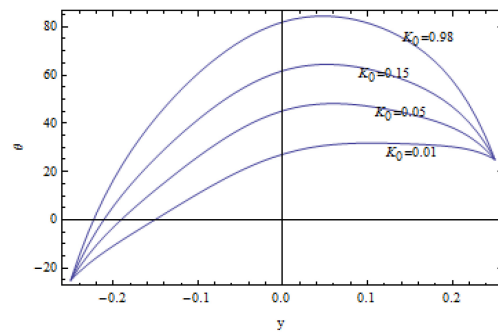


**Figure 23.** The temperature of the fluid is drawn against  $y$  for different values of  $K_0 = 0.01, 0.05, 0.15, 0.98$ ,  $Q = 5$ ,  $M = 0.1$ ,  $\lambda = 0.5$ ,  $G_R = 200$ ,  $R_T = 50$ ,  $\varepsilon = 8$ ,  $B_r = 0.5$ .

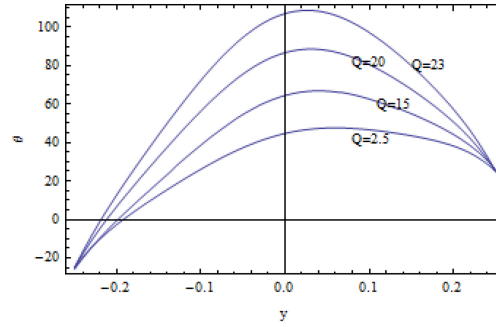


**Figure 24.** The temperature of the fluid is drawn against  $y$  for different values of  $Q = 2.5, 15, 20, 23$ ,  $K_0 = 0.01$ ,  $M = 0.01$ ,  $\lambda = 0.01$ ,  $G_R = 200$ ,  $R_T = 50$ ,  $\varepsilon = 8$ ,  $B_r = 0.5$ .

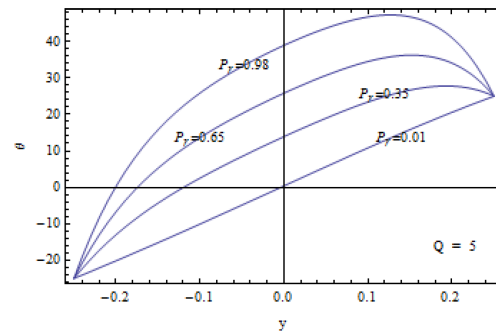


**Figure 25.** The temperature of the fluid is drawn against  $y$  for different values of  $Pr = 0.01, 0.35, 0.65, 0.98$ ,  $\lambda = 0.9$ ,  $M = 5$ ,  $K_0 = 0.09$ ,  $B_r = 1$ ,  $R_T = 50$ ,  $G_R = 400$ ,  $L = 1$ ,  $Q = 5$ ,  $Re = 0.55$ .

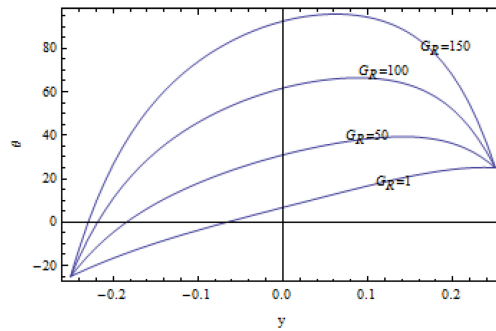


**Figure 26.** The temperature of the fluid is drawn against  $y$  for different values of  $G_R = 1, 50, 100, 150$ ,  $K_0 = 0.01$ ,  $M = 0.1$ ,  $\lambda = 0.01$ ,  $Q = 2.5$ ,  $R_T = 50$ ,  $\varepsilon = 8$ ,  $B_r = 0.5$ .



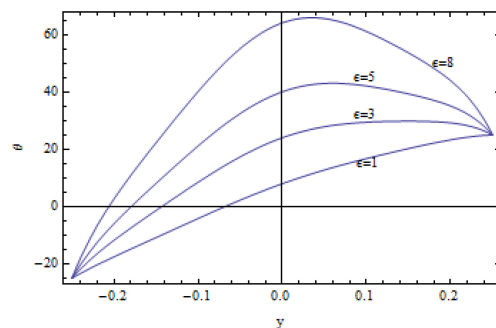


**Figure 27.** The temperature of the fluid is drawn against  $y$  for different values of  $\varepsilon = 1, 3, 5, 8$ ,  $K_0 = 0.01$ ,  $M = 0.1$ ,  $\lambda = 0.01$ ,  $Q = 5$ ,  $R_T = 50$ ,  $G_R = 300$ ,  $B_r = 0.1$ .

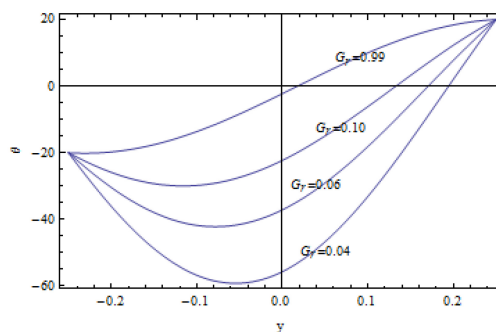


**Figure 28.** The temperature of the fluid is drawn against  $y$  for different values of  $G_r = 0.04, 0.06, 0.10, 0.99$ ,  $\lambda = 0.09$ ,  $M = 0.1$ ,  $K_0 = 0.01$ ,  $B_r = 0.01$ ,  $\varepsilon = 0.01$ ,  $Q = 40$ ,  $R_e = 5$ ,  $R_T = 40$ .

### References

- [1] N. T. M. Eldabe and Oaf, Darcy-Lap wood-Brinkman fluid flow and heat transfer through porous medium over a stretching porous sheet, Bull. Cal. Math. Soc. 92(2) (2000), 133-142.
- [2] N. T. M. Eldabe, G. M. Moatimid and H. S. Ali, Magnetohydrodynamic flow of non-Newtonian viscoelastic fluid through a porous medium near an accelerated plate, Can. J. Phys. 81 (2003), 1249-1269.
- [3] N. T. M. Eldabe, M. A. Mahmoud and Gamal M. A. El Rahman, Unsteady magnetic boundary layer flow of power law non-Newtonian conducting fluid through a porous medium past an infinite porous flat plate, Astrophysics and Space Science 178 (1991), 197-204.

- [4] N. T. M. Eldabe and S. N. Sallam, Non-Darcy Couette flow through a porous medium of magnetohydrodynamic viscoelastic fluid with heat and mass transfer, *Can. J. Phys.* 83 (2005), 1241-1263.
- [5] S. M. M. El-Kabeir, M. A. El-Hakiem and A. M. Rashad, Lie group analysis of unsteady MHD three dimensional by natural convection from an inclined stretching surface saturated porous medium, *J. Comput. Appl. Math.* 213 (2008), 582-603.
- [6] A. J. Chamkha, Hydromagnetic three-dimensional free convection on a vertical stretching surface with heat generation or absorption, *Internat. J. Heat Fluid Flow* 20 (1999), 84-92.
- [7] A. J. Chamkha, Transient hydromagnetic three-dimensional natural convection from an inclined stretching permeable surface, *Chem. Engng. J.* 76 (2000), 159-168.
- [8] T. C. Chiam, Hydromagnetic flow over a surface stretching with a power-law velocity, *Internat. J. Engng. Sci.* 33 (1995), 429-435.
- [9] K. Vajravelu and A. Hadjinicolaou, Convective heat transfer in an electrically conducting fluid at a stretching surface with uniform free stream, *Internat. J. Engng. Sci.* 35 (1997), 1237-1244.
- [10] M. Yurusoy and M. Pakdemirli, Exact solutions of boundary layer equations of a special non-Newtonian fluid over a stretching sheet, *Mech. Res. Commun.* 26 (1999), 171-175.
- [11] A. Ishak and R. Nazar Pop I, Hydromagnetic flow and heat transfer adjacent to a stretching vertical sheet, *Heat Mass Transfer* 44 (2008), 921-927.
- [12] Subhas Abel, K. V. Prasad and Ali Mahaboob, Buoyancy force and thermal radiation effects in MHD boundary layer visco-elastic fluid flow over continuously moving stretching surface, *Int. J. Therm. Sci.* 44 (2005), 465-476.
- [13] N. T. M. Eldabe and S. M. G. Elmohands, Heat transfer of MHD non-Newtonian Casson fluid flow between two rotating cylinders, *J. Phys. Soc. Japan* 64(11) (1995), 4164.
- [14] J. Boyd, J. M. Buick and S. Green, Analysis of the Casson and Carreau-Yasuda non-Newtonian blood models in steady and oscillatory flow using the lattice Boltzmann method, *Phys. Fluids* 19 (2007), 93-103.
- [15] Ming-I Char, Heat and mass transfer in a hydromagnetic flow of the viscoelastic fluid over a stretching sheet, *J. Math. Anal. Appl.* 186 (1994), 674-689.
- [16] M. Nakamura and T. Sawada, Numerical study on the flow of a non-Newtonian fluid through an axisymmetric stenosis, *ASME J. Biomechanical Engineering* 110(2) (1988), 137-143.

- [17] J. C. Umavathi and M. S. Malashetty, Magnetohydrodynamic mixed convection in a vertical channel, *Int. J. Non-Linear Mechanics* 40 (2005), 91-101.
- [18] M. J. Lighthill, *Proc. R. Soc. London A* 224 (1) 1955.